Intracellular position of mitochondria and chloroplasts in bundle sheath and mesophyll cells of C$_3$ grasses in relation to photorespiratory CO$_2$ loss

Yuto Hatakeyama & Osamu Ueno

REGULAR PAPER

OPEN ACCESS

Intracellular position of mitochondria and chloroplasts in bundle sheath and mesophyll cells of C$_3$ grasses in relation to photorespiratory CO$_2$ loss

Yuto Hatakeyama[a] and Osamu Ueno[a,b]

[a]Graduate School of Bioresources and Bioenvironmental Sciences, Kyushu University, Fukuoka, Japan; [b]Faculty of Agriculture, Kyushu University, Fukuoka, Japan

ABSTRACT

In C$_3$ plants, photosynthetic efficiency is reduced by photorespiration. A part of CO$_2$ fixed during photosynthesis in chloroplasts is lost from mitochondria during photorespiration by decarboxylation of glycine by glycine decarboxylase (GDC). Thus, the intracellular position of mitochondria in photosynthetic cells is critical to the rate of photorespiratory CO$_2$ loss. We investigated the intracellular position of mitochondria in parenchyma sheath (PS) and mesophyll cells of 10 C$_3$ grasses from 3 subfamilies (Ehrhartoideae, Panicoideae, and Pooideae) by immunostaining for GDC and light and electron microscopic observation. Immunostaining suggested that many mitochondria were located in the inner half of PS cells and on the vacuole side of chloroplasts in mesophyll cells. Organelle quantification showed that 62–75% of PS mitochondria were located in the inner half of cells, and 62–78% of PS chloroplasts were in the outer half. In mesophyll cells, 61–92% of mitochondria were positioned on the vacuole side of chloroplasts and stromules. In PS cells, such location would reduce the loss of photorespiratory CO$_2$ by lengthening the path of CO$_2$ diffusion and allow more efficient fixation of CO$_2$ from intercellular spaces. In mesophyll cells, it would facilitate scavenging by chloroplasts of photorespiratory CO$_2$ released from mitochondria. Our data suggest that the PS cells of C$_3$ grasses have already acquired an initial structure leading to proto-Kranz and further C$_3$–C$_4$ intermediate anatomy. We also found that in the Pooideae, organelle positioning in PS cells on the phloem side resembles that in mesophyll cells.

Introduction

Photorespiration reduces photosynthetic efficiency of C$_3$ plants, particularly at high temperature with low CO$_2$ concentration. In rice, a staple crop worldwide, reduction of photosynthesis by photorespiration is estimated to be 25–35% at 30–35 °C at current CO$_2$ levels (Sage, 2001). Therefore, the suppression of photorespiration is an important target to improve crop productivity. The first reaction of photorespiration is oxidation of ribulose 1,5-bisphosphate by ribulose 1,5-bisphosphate carboxylase/oxygenase (rubisco); phosphoglycolate generated by this reaction is metabolized in the glycolate pathway, which requires cooperation between chloroplasts, peroxisomes, and mitochondria. Glycine generated in peroxisomes is transported to mitochondria, where it is decarboxylated by glycine decarboxylase (GDC) (Bauwe, 2011; Douce et al., 2001).

In higher plants, the C$_4$ photosynthetic pathway is the most efficient mechanism that reduces photorespiration; C$_4$ plants are thought to have evolved from C$_3$ plants primarily in response to a decline in atmospheric CO$_2$ concentrations that began during the Cretaceous and continued until the Miocene (Ehleringer et al., 1991). The leaves of most C$_4$ plants show Kranz type leaf anatomy characterized by two types of photosynthetic cells – mesophyll and bundle sheath (BS) cells – and photorespiration is repressed by concentrating CO$_2$ around rubisco in chloroplasts of BS cells (Hatch, 1987). As a result, C$_4$ plants retain high photosynthetic capacity even in environments that cause high photorespiration (Ehleringer et al., 1991).

There are plants having photosynthetic characteristics intermediate between those of C$_3$ and C$_4$ plants, which are called C$_3$–C$_4$ intermediate plants (Edwards & Ku, 1987). Their leaf anatomy and CO$_2$ exchange characteristics such as CO$_2$ compensation points and O$_2$ inhibition of photosynthesis are in between those of C$_3$ and C$_4$ plants. Low rates of photorespiration in C$_3$–C$_4$ intermediates result mainly from the intercellular localization of GDC (Monson & Rawsthorne, 2000; Rawsthorne, 1992). C$_3$–C$_4$ intermediate plants are considered to be an intermediate stage in

CONTACT Osamu Ueno ✉ uenoos@agr.kyushu-u.ac.jp

Supplemental data for this article can be accessed here.

the evolution of C_4 plants from C_3 ancestors (Edwards & Ku, 1987; Monson & Rawsthorne, 2000; Sage et al., 2014). The repositioning and enhancement of mitochondria and chloroplasts in BS cells and the BS-specific expression of GDC are important for the establishment of C_3–C_4 intermediate photosynthesis. However, the C_3 cycle operates in both M and BS cells of C_3–C_4 intermediates (Edwards & Ku, 1987; Monson & Rawsthorne, 2000).

Recently, the early stage of evolution of C_3–C_4 intermediate plants from C_3 plants was termed proto-Kranz (Muhaidat et al., 2011; Sage et al., 2013, 2014). Leaf anatomy of proto-Kranz plants resembles that of C_3–C_4 intermediates, but GDC accumulates in both mesophyll and BS mitochondria. Proto-Kranz plants still perform C_3 photosynthesis, but many mitochondria in their BS cells are located along the inner tangential walls adjacent to the vascular bundle. Some chloroplasts cover these mitochondria and therefore may capture some of photorespiratory CO_2 released from BS mitochondria. Proto-Kranz species have been found in some genera such as *Panicum* and *Steinchisma* in the Poaceae (Brown et al., 1983; Sage et al., 2014), *Flaveria* in the Asteraceae (Sage et al., 2013), *Heliotropium* in the Boraginaceae (Muhaidat et al., 2011; Vogan et al., 2007), and *Salsola* in the Chenopodiaceae (Voznesenskaya et al., 2013). However, it is unclear whether proto-Kranz species are common in other groups. It is also unknown whether organelles are scattered randomly or are positioned according to some rules in the BS cells of C_3 plants. This information is important for understanding early steps of evolution of photosynthetic types.

Some C_3 plants restrict photorespiratory CO_2 efflux without alterations in their biochemistry (Buchner et al., 2015; Moser et al., 2015; Sage & Sage, 2009). Sage and Sage (2009) observed that in rice mesophyll cells, much of the cell periphery is occupied by chloroplasts and their protrusions (stromules) filled with stroma containing rubisco (Bourett et al., 1999; Gray et al., 2001). Stromules may efficiently refix some CO_2 released from mitochondria, and it is important for the mitochondria in mesophyll cells to be located on the vacuole side of the chloroplasts and stromules. However, information about the position of mitochondria in mesophyll cells of C_3 grasses is scarce.

In this study, we investigated intracellular positioning of mitochondria and chloroplasts in parenchyma sheath (PS) and mesophyll cells of 10 C_3 species from 3 subfamilies of the grass family (Ehrhartoideae, Panicoideae, and Pooideae) using *in situ* immunostaining of GDC and light and electron microscopic observation. The Ehrhartoideae (formerly Oryzoideae) is a C_3 subfamily occurring mainly in tropical and subtropical regions, whereas the Pooideae is a C_3 subfamily thriving mainly in cool temperate regions. The Panicoideae includes both C_3 and C_4 species and is distributed in tropical and subtropical regions (Grass

Phylogeny Working Group, 2001; Edwards & Smith, 2010). Our results reveal that positioning of the organelles that leads to proto-Kranz anatomy is already present in PS cells of these C_3 grasses. In addition, we confirmed that many mitochondria in mesophyll cells are positioned on the vacuole side of chloroplasts and suggest that the mechanism of scavenging photorespiratory CO_2 proposed for rice and wheat (Sage & Sage, 2009) also exists in other C_3 grasses.

Materials and Methods

Plant materials and growth

We investigated 10 C_3 species of 8 genera from 3 grass subfamilies: *Oryza alta* Swallen (W0017), *Oryza glaberrima* Steud. (cv. TOG 8,000), and *Oryza sativa* L. (cv. Nipponbare) in the Ehrhartoideae; *Oplismenus undulatifolius* (Ard.) Roem. et Schult. and *Panicum bisulcatum* Thunb. in the Panicoideae; and *Avena fatua* L., *Bromus catharticus* Vahl, *Bromus rigidus* Roth, *Lolium perenne* L., and *Triticum aestivum* L. in the Pooideae. The three *Oryza* species and *T. aestivum* were grown from seeds in 5-L pots containing sandy soil. The seeds of *O. alta* were provided by the National Institute of Genetics, Mishima, Japan. The seeds of *O. glaberrima* were provided by the Gene Bank Laboratory of the Genetic Resource Center, National Institute of Agrobiological Sciences, Tsukuba, Japan. Young plants of *O. undulatifolius* and *P. bisulcatum* were collected on sunny places in the Hakozaki campus of Kyusyu University, Fukuoka, Japan, and transplanted into 5-L pots containing sandy soil. Fertilizer containing 0.6 g of each N [as $(NH_4)_2SO_4$], P [as $Ca(H_2PO_4)_2$], and K [as KCl] was supplied to soil in pots. The three species of *Oryza* and the two species of the Panicoideae were grown in a greenhouse [natural sunlight, wherein photosynthetic photon flux density (PPFD) at midday exceeded 1,500 μmol m^{-2} s^{-1}; minimum and maximum temperatures, 25 °C and 35 °C] for about 6 weeks in August and September, 2014. *Triticum aestivum* was grown in a growth chamber (natural sunlight, wherein PPFD at midday exceeded 1000 μmol m^{-2} s^{-1}; 25 °C; relative humidity, 70%) for about 8 weeks. The remaining four species of the Pooideae were collected on sunny places (maximum PPFD, about 1,400 μmol m^{-2} s^{-1}) in the Hakozaki campus of Kyusyu University in April 2014, and the leaves were immediately used for experiments.

Visualization of mitochondria by immunostaining of the P-protein of GDC

The photorespiratory enzyme GDC is a major protein in the mitochondria of photosynthetic cells of C_3 plants (Douce et al., 2001). Therefore, we visualized the mitochondria in mesophyll and BS cells of C_3 grass leaves by

immunohistochemical staining of the P-protein of GDC and observed them under a light microscope. Fully expanded uppermost leaves were sampled from three plants of each species at 09:00 on a sunny day and fixed within 30 min. Segments from the middle of the leaves were fixed with 3% (w/v) paraformaldehyde / 0.2% (v/v) glutaraldehyde in 50 mM sodium phosphate (pH 6.8) for 10 h at 4 °C and then washed in phosphate buffer (pH 6.8). Fixed tissues were dehydrated through an ethanol/butanol series, infiltrated with 100% butanol overnight at room temperature, and incubated in a 1:1 mixture of butanol : Paraplast (Paraplast X-TRA, Fisher Scientific Co., Houston, TX, USA) for 1 day at 56 °C. Samples were then infiltrated with pure Paraplast for 8 h at 56 °C and in fresh Paraplast overnight at 56 °C. Finally, samples were embedded in fresh Paraplast. Transverse sections (8 μm thick) were cut on a microtome (Yamato Koki Co.,Ltd., Saitama, Japan), mounted on slides coated with poly-L-lysine (Sigma-Aldrich, Inc., St. Louis, MO, USA) and dried overnight at 46 °C.

Slides were immersed in xylene to remove the Paraplast and the sections on the slides were rehydrated through an ethanol series. The sections were incubated with 0.1% (w/v) trypsin for 30 min and then with 5% (v/v) hydrogen peroxide for 1 h, rinsed with distilled water and 10 mM phosphate buffer (pH 7.2) containing 150 mM NaCl (PBS), and incubated with 5% (w/v) bovine serum albumin (BSA) in PBS for 10 min. The sections were then incubated with antiserum against the P-protein of GDC of pea leaf mitochondria diluted 1:2000 with PBS containing 1% (w/v) BSA for 1 h at room temperature. The antiserum was provided by Prof. D. J. Oliver (University of Idaho, Moscow, ID, USA); the same antiserum was used in our previous studies of grasses (Yoshimura et al., 2004) and crucifers (Ueno, 2011; Ueno et al., 2003). The sections were rinsed with distilled water and PBS, incubated with a secondary antibody (anti-rabbit goat antibody conjugated with horseradish peroxidase; American Qualex, San Clemente, CA, USA) diluted 1:100 with PBS containing 1% (w/v) BSA for 30 min, and rinsed with distilled water and PBS. Finally, the P-protein in the sections was visualized by use of Peroxidase-Stain-DAB (3,3-diaminobenzidine tetrahydrochloride) Kit (Nacalai Tesque, Inc., Kyoto, Japan). The sections were observed under a light microscope.

Leaf anatomy and ultrastructure

Segments from the middle of fully expanded uppermost leaves collected from three plants of each species on a sunny day were fixed in 3% (v/v) glutaraldehyde in 50 mM sodium phosphate buffer (pH 6.8) at room temperature for 2 h, washed with phosphate buffer, postfixed with 2% (v/v) OsO_4 in 50 mM phosphate (pH 6.8) buffer for 2 h, dehydrated through an acetone series, and embedded in

Spurr's resin. For light microscopy, semi-thin sections were cut with a glass knife and stained with 1% (w/v) toluidine blue O. For electron microscopy, ultra-thin sections were cut with a diamond knife and stained with lead citrate. They were observed under an electron microscope (JEM-100CX II K, JEOL Ltd., Tokyo, Japan) at 75 kV.

Quantification of mitochondria and chloroplasts

We recorded the numbers and intracellular positions of mitochondria and chloroplasts in 28 to 40 mesophyll cells and PS cells (outer BS cells surrounding the vascular bundle) of small vascular bundles (Chonan et al., 1974) selected from leaves of three plants under the electron microscope. In PS cells, we counted the numbers of organelles positioned in the inner half of cells (i.e. in the inner tangential walls and the inner half of the radial walls of cells) and in the outer half of cells (i.e. in the outer tangential walls and the outer half of the radial walls of cells) (Figure 6). In general, PS cells are round in transverse section. However, those of irregular shape were excluded from measurement. In mesophyll cells, we counted the mitochondria on the vacuole side of chloroplasts (inner position) and on the cell wall side of chloroplasts including isolated mitochondria not associated with chloroplasts but adjacent to the cell wall (outer position; Figure 6); equal numbers of mesophyll cells were selected from abaxial and adaxial sides. Simultaneously, we counted the chloroplasts in mesophyll cells. We also evaluated the position of mitochondria in L-type PS cells (Williams et al., 1989 and see Results for details) of the Pooideae as for mesophyll cells.

Statistical analysis

Student's t-test was used to test the significance ($p < 0.05$) of the differences between the proportions of mitochondria or chloroplasts located in the centripetal and centrifugal positions in PS cells and the differences between the proportions of mitochondria located in the inner and outer positions in mesophyll cells and L-type PS cells.

Results

Light microscopic observation of leaf structure

In leaves of C_3 grasses, the vascular bundle is generally surrounded by two layers of BS: outer PS and inner mestome sheath (MS) (Brown, 1975). In small vascular bundles of rice, however, the MS is not obvious (Kaneko et al., 1980). We found similar features in the C_3 species of the Ehrhartoideae and Panicoideae (Figure 1(A)–(D)). In the C_3 species of the Pooideae, vascular bundles were surrounded by both PS and MS (Figure 1(E)–(H)). The mesophyll cells
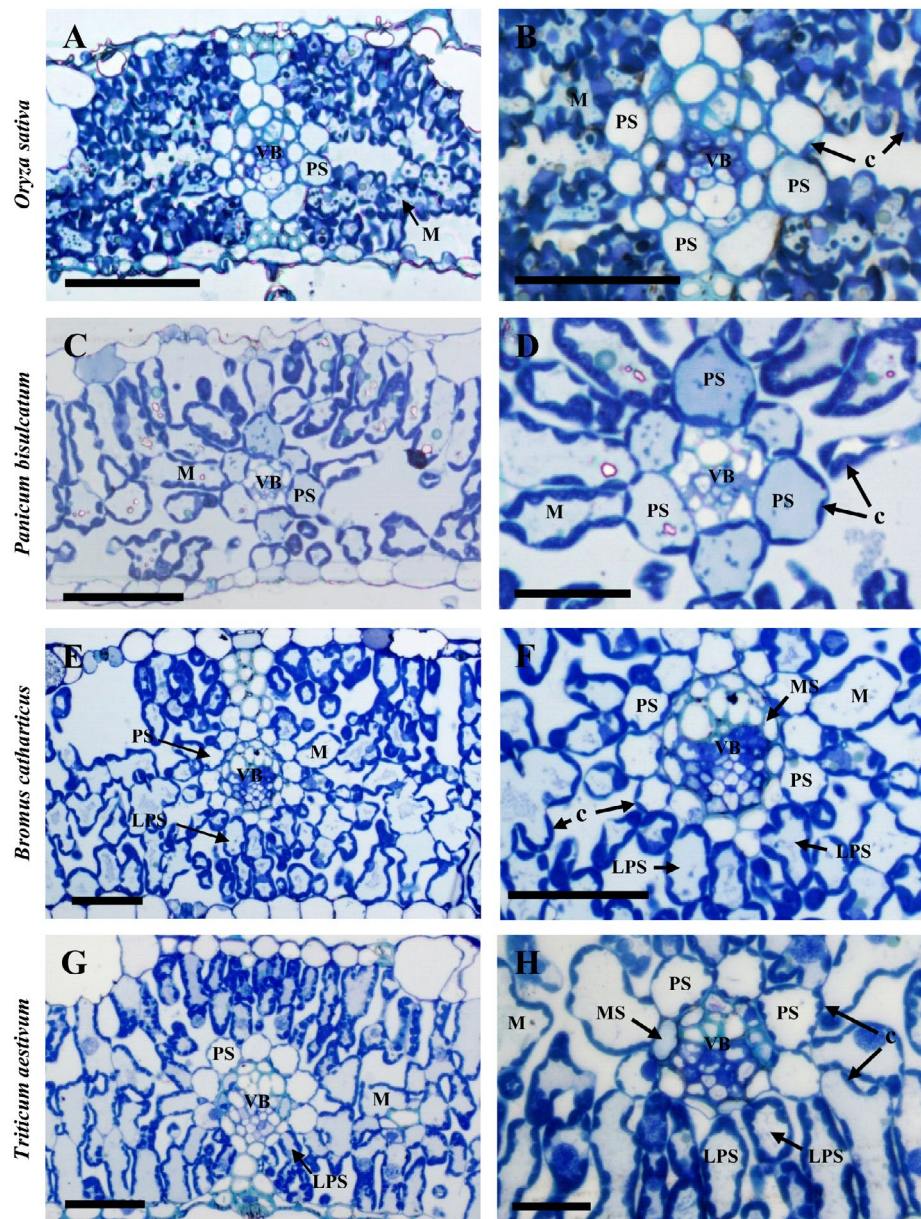
Figure 1. Cross sections of leaves of (A, B) *Oryza sativa*, (C, D) *Panicum bisulcatum*, (E, F) *Bromus catharticus*, and (G, H) *Triticum aestivum*.
Notes. LPS, L-type parenchyma sheath cell; M, mesophyll cell; MS, mestome sheath cell; PS, ordinary parenchyma sheath cell; VB, vascular bundle; c, chloroplast.
Bars = 50 μm.

of *Oryza* species had many lobes, which is a characteristic of armed cells (Chonan, 1970; Sage & Sage, 2009). In the mesophyll of *Oryza*, cells were densely arranged and intercellular spaces were small (Figure 1(A)). Intercellular spaces were larger in the Panicoideae and Pooideae than in the Ehrhartoideae (Figure 1(C), (E) and (G)). The PS cells of the Ehrhartoideae contained few chloroplasts (Figure 1(B)), whereas those of the Panicoideae and Pooideae contained many (Figure 1(D), (F) and (H)). In the Pooideae, the PS cells on the phloem side of the bundle differed structurally from those on the xylem side and were similar in their appearance to mesophyll cells (Figure 1(E)–(H)). We call the PS cells on the phloem side 'L-type' PS cells and distinguish

them from 'ordinary' PS cells (according to the terminology of Williams et al., 1989). Ordinary PS cells contained fewer chloroplasts than mesophyll cells, whereas L-type PS cells had similar numbers of chloroplasts.

Light microscopic observation of mitochondria by GDC immunostaining

In all grasses examined, immunohistochemical staining of the P-protein of GDC revealed the mitochondria in PS and mesophyll cells as reddish brown granules under a light microscope (Figure 2). However, some mesophyll cells of the Ehrhartoideae showed almost no staining
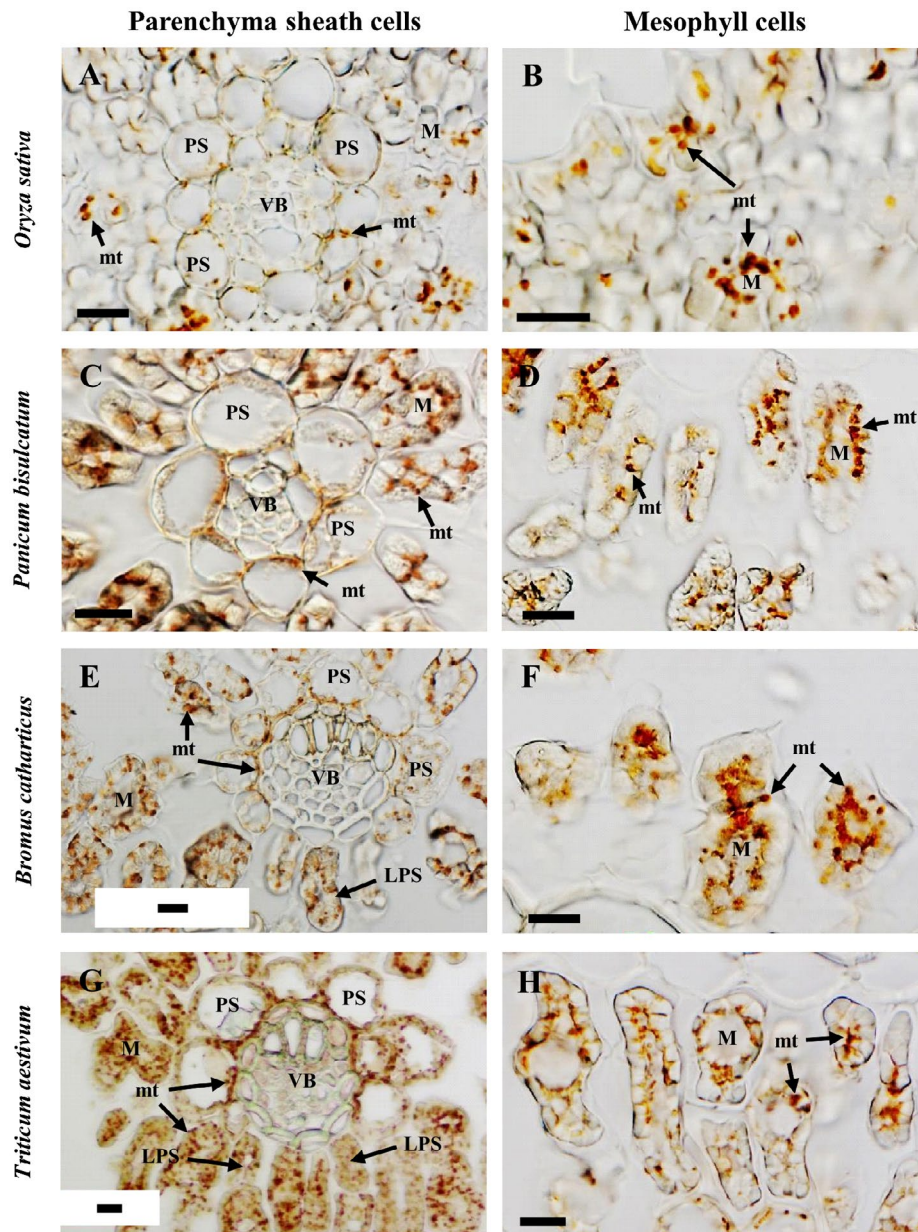
Parenchyma sheath cells   **Mesophyll cells**

Figure 2. *In situ* immunolocalization of the P-protein of glycine decarboxylase in leaves of (A, B) *O. sativa*, (C, D) *P. bisulcatum*, (E, F) *B. catharticus*, and (G, H) *T. aestivum*.
Notes. LPS, L-type parenchyma sheath cell; M, mesophyll cell; PS, ordinary parenchyma sheath cell; VB, vascular bundle; mt, mitochondrion. Bars = 10 µm.

(Figure 2(B)), probably because the cell walls of mesophyll cells in *Oryza* species are thicker than those of other grasses, which may have impeded the diffusion of the antibody, color development solution, or both into mesophyll cells.

In the PS cells, the number of mitochondria differed between species. The PS cells of the Panicoideae and ordinary PS cells of the Pooideae contained relatively many mitochondria, which were positioned along the inner tangential cell walls, forming a band around the vascular bundle (Figure 2(C), (E) and (G). In the Ehrhartoideae, PS cells contained only few mitochondria, which were scattered within the cell (Figure 2(A)).

In the mesophyll cells of all C_3 grasses examined, many mitochondria were positioned on the vacuole side of chloroplasts (Figure 2(B), (D), (F) and (H)). In the L-type PS cells of the Pooideae, the position of mitochondria was similar to that in mesophyll cells, and no centripetal positioning of mitochondria were found, unlike in ordinary PS cells (Figure 2(E) and (G)).

Ultrastructural observation and quantification of mitochondria and chloroplasts

In the PS cells of all C_3 grasses except *A. fatua*, a significantly higher proportion of mitochondria (64–75%) was found in

Table 1. Intracellular position and number of mitochondria and chloroplasts in parenchyma sheath cells of C_3 grasses.

Subfamily	Species	Mitochondria			Chloroplasts		
		Outer half of cell (%)	Inner half of cell (%)	Number per cell profile	Outer half of cell (%)	Inner half of cell (%)	Number per cell profile
Ehrhartoideae	*Oryza alta*	34.6 ± 5.0	65.4 ± 5.0*	3.8 ± 0.9	62.3 ± 11.8	37.7 ± 11.8	2.2 ± 0.1
	O. glaberrima	25.4 ± 1.5	74.6 ± 1.5*	2.3 ± 0.7	75.4 ± 2.0	24.6 ± 2.0*	1.2 ± 0.2
	O. sativa	28.8 ± 8.6	71.2 ± 8.6*	2.5 ± 1.1	69.0 ± 5.3	31.0 ± 5.3*	1.4 ± 0.2
Panicoideae	*Oplismenus undulatifolius*	27.2 ± 3.2	72.8 ± 3.2*	7.4 ± 0.5	64.6 ± 2.2	35.4 ± 2.2*	3.7 ± 0.5
	Panicum bisulcatum	35.7 ± 2.6	64.3 ± 2.6*	9.6 ± 2.1	63.6 ± 4.4	36.4 ± 4.4*	4.2 ± 0.3
Pooideae	*Avena fatua*	37.7 ± 15.1	62.3 ± 15.1	4.9 ± 1.4	77.7 ± 1.0	22.3 ± 1.0*	6.7 ± 1.7
	Bromus catharticus	31.8 ± 4.7	68.2 ± 4.7*	6.7 ± 0.8	68.8 ± 17.8	31.2 ± 17.8	7.8 ± 0.7
	B. rigidus	26.0 ± 7.4	74.0 ± 7.4*	9.6 ± 1.5	66.8 ± 2.9	33.2 ± 2.9*	5.8 ± 1.0
	Lolium perenne	35.6 ± 5.3	64.4 ± 5.3*	6.7 ± 1.2	67.8 ± 4.5	32.2 ± 4.5*	6.3 ± 1.6
	Triticum aestivum	29.3 ± 8.1	70.7 ± 8.1*	6.7 ± 0.8	62.9 ± 3.5	37.1 ± 3.5*	4.3 ± 0.5

Notes. Values are means ± SD of three plants.
See Figure 6 for the position of organelles in the outer and inner half of cell.
For the Pooideae, data for ordinary parenchyma sheath cells are shown.
* indicate significant differences between the two positions of organelles ($p < 0.05$).

the centripetal than in the centrifugal position (Table 1). In *A. fatua*, 62% of mitochondria were found in the centripetal position, although the difference was not significant (Table 1). In contrast, a significantly higher proportion of chloroplasts (63–78%) was found in the centrifugal than in the centripetal position in the PS cells of all C_3 grasses except *O. alta* and *B. catharticus* (Table 1). In the latter two species, 62–69% of chloroplasts were in the centrifugal position, but the difference was not significant. Centrifugally positioned mitochondria generally occurred near chloroplasts (Figure 3(C), (E), and (G)), whereas some centripetal mitochondria were not associated with chloroplasts (Figure 3(B), (D), (F), and (H)). In *P. bisulcatum*, *B. catharticus*, and *T. aestivum*, mitochondria covered by chloroplasts were occasionally observed along the inner tangential walls of PS cells (Suppl. data 1). In *B. catharticus* and *T. aestivum*, mitochondria covered by chloroplasts occurred only in the vicinity of plasmodesmata (Suppl. data 1B, C).

In the mesophyll cells of all grasses except for *B. rigidus*, 68–92% of mitochondria were positioned on the vacuole side of chloroplasts (Figure 4, Table 2). (In *B. rigidus*, this value was 61%, although the difference was not significant; Table 2). Mitochondria located close to cell walls and not associated with chloroplasts were rare, although some mitochondria were located in the gaps between chloroplasts (Figure 4(D)); these mitochondria were counted as located in the outer position. In *B. rigidus*, the gaps between chloroplasts were large because chloroplasts were sparse, and thus many mitochondria were located in the gaps, being adjacent to the cell wall (Suppl. data 2A). Stromules were observed in the mesophyll cells of all C_3 grasses (Figure 4(B), (F) and (H)), but rarely in the PS cells (Figure 3(H)). In the mesophyll cells of the three *Oryza* species, stromules were well developed (Figure 4(B)). When *O. undulatifolius* (Panicoideae) was compared with *P. bisulcatum* belonging to the same subfamily, the proportion of

mitochondria located in the inner position was higher in the former (92%) than in the latter (68%). This was because the mesophyll chloroplasts of *O. undulatifolius* (Suppl. data 2B) have more-developed stromules than those of *P. bisulcatum* (Figure 4(C) and (D)).

The intracellular positioning of mitochondria in L-type PS cells of the Pooideae was evaluated as for mesophyll cells, because these cell types are structurally similar (Figure 5). In the L-type PS cells of all pooid grasses except for *B. rigidus*, 68–88% of mitochondria were positioned on the vacuole side of chloroplasts (Figure 5; Table 3). In *B. rigidus*, the proportion of mitochondria in the outer and inner positions was almost the same (Table 3). L-type PS cells contained fewer mitochondria and chloroplasts per cell (Table 3) than mesophyll cells (Table 2).

Discussion

This study investigated the intracellular positions of mitochondria and chloroplasts in the PS and mesophyll cells of leaves of 10 C_3 grass species from 3 different subfamilies. These organelles showed unique positioning related to photosynthetic and photorespiratory functions.

Intracellular position of mitochondria and chloroplasts in PS cells

In the PS cells (except the L-type) of C_3 grasses, 62–75% of mitochondria and 22–38% of chloroplasts were located in the inner half of cells (Table 1). These values were lower than those reported for the proto-Kranz species of *Heliotropium* (Muhaidat et al., 2011) and *Flaveria* (Sage et al., 2013), which are considered to represent an early stage of evolution of C_3–C_4 intermediates from C_3 plants. Our data show that the organelle positioning found in the PS cells is common to C_3 grasses. The evolutionary origin of the proto-Kranz type would result from the structural
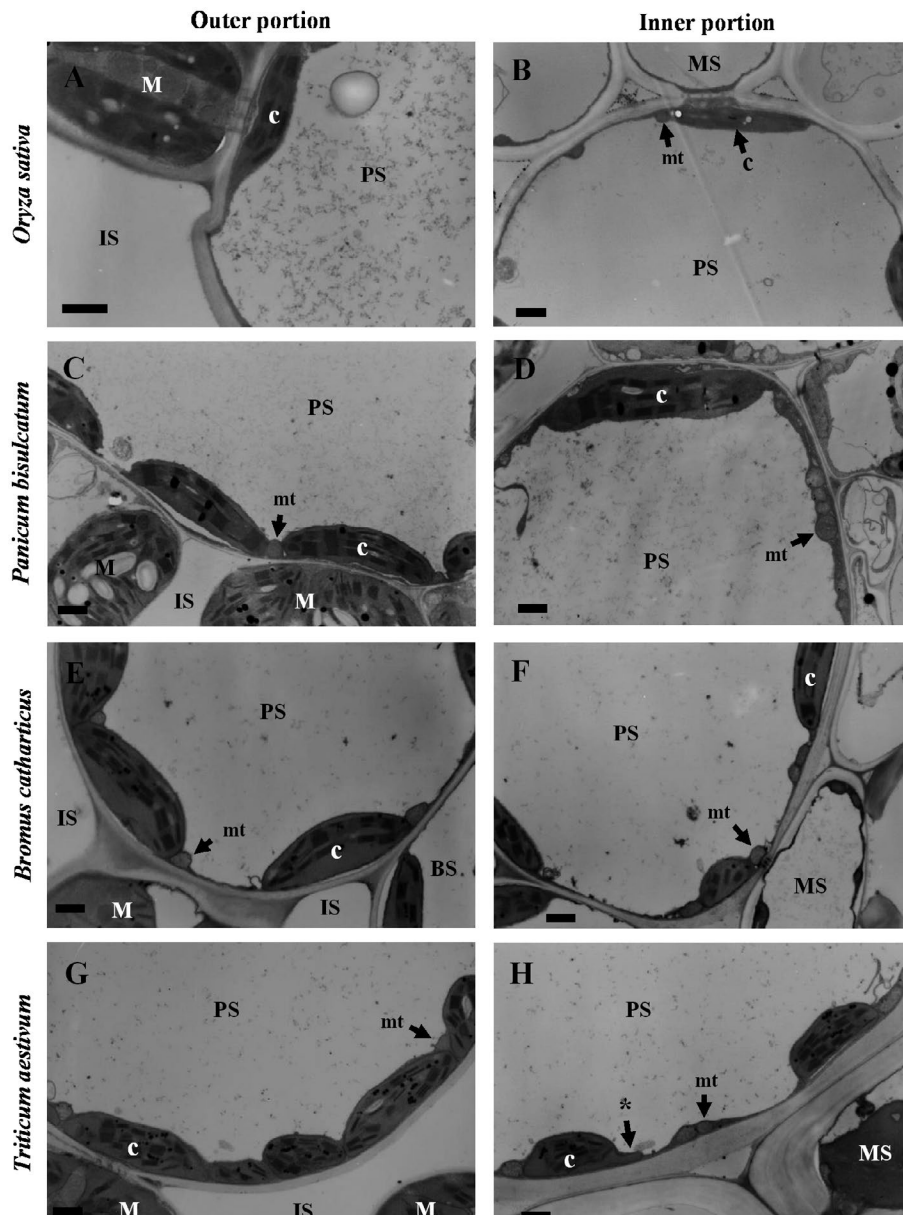
Figure 3. Ultrastructure of parenchyma sheath cells in (A, B) *O. sativa*, (C, D) *P. bisulcatum*, (E, F) *B. catharticus*, and (G, H) *T. aestivum*. (A, C, E, G) Outer and (B, D, F, H) inner portions of the cells are shown.
Notes. IS, intercellular space; M, mesophyll cell; MS, mestome sheath cell; PS, ordinary parenchyma sheath cell; c, chloroplast; mt, mitochondrion; *, chloroplast protrusion (stromule). Bars = 1 µm.

feature existing in the PS cells of C₃ grasses. Although there are several studies on the ultrastructure of PS cells in C₃ grasses (Brown et al., 1983; Carolin et al., 1973; Kaneko et al., 1980; Sage & Sage, 2009), they made no mention of the organelle positioning. We consider that it would be difficult to find the particular positioning of organelles without the immunostaining of GDC and the quantification of organelles.

An interesting question is what is the physiological significance of this organelle distribution in the PS cells of C₃ grasses. Photosynthetic and photorespiratory activities of these cells are much lower than those of mesophyll cells, as estimated from the numbers of chloroplasts and

mitochondria (Leegood, 2008; Yoshimura et al., 2004). Yet the PS cells of C₃ grasses appear to position organelles to fix CO₂ most effectively (Figure 6). Centrifugal chloroplast location may be advantageous for efficient fixation of CO₂ from intercellular spaces (Sage et al., 2014; Ueno, 2011; Ueno et al., 2003). In terms of carbon economy, it may be better to fix intercellular CO₂ rather than CO₂ generated in vascular tissue. Because CO₂ is produced in mitochondria, the centripetal location of mitochondria in PS cells may reduce the loss of photorespiratory (and respiratory) CO₂ by lengthening the path of CO₂ diffusion (Figure 6). In the PS cells of some C₃ grasses, mitochondria were covered by chloroplasts, especially in the vicinity of plasmodesmata
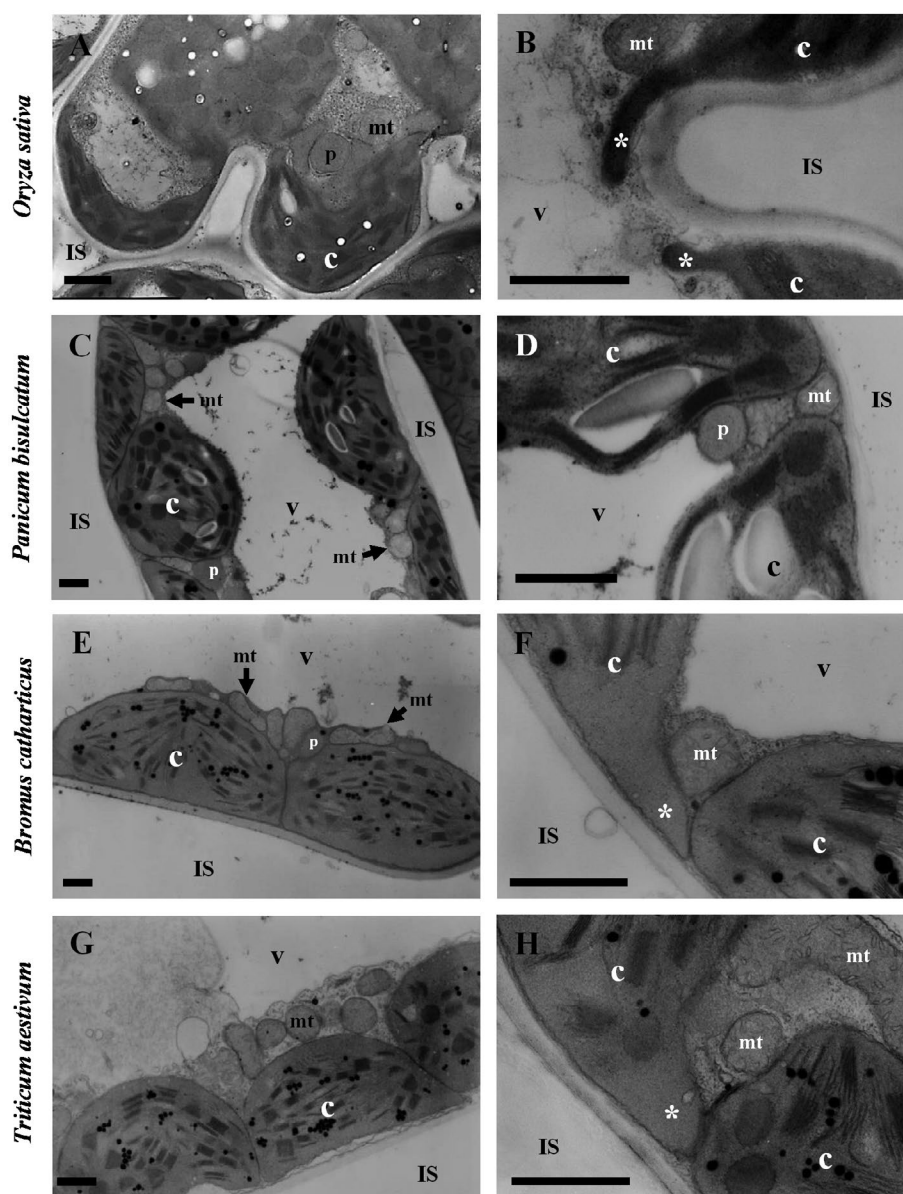
Figure 4. Ultrastructure of mesophyll cells in (A, B) *O. sativa*, (C, D) *P. bisulcatum*, (E, F) *B. catharticus*, and (G, H) *T. aestivum*.
Notes. IS, intercellular space; c, chloroplast; mt, mitochondrion; p, peroxisome; v, vacuole; *, chloroplast protrusions (stromules). Bars = 1 μm.

Table 2. Intracellular position and number of mitochondria and chloroplasts in mesophyll cells of C$_3$ grasses.

Subfamily	Species	Mitochondria			Chloroplasts (number per cell profile)
		Outer position (%)	Inner position (%)	Number per cell profile	
Ehrhartoideae	*Oryza alta*	14.1 ± 6.8	85.9 ± 6.8*	6.8 ± 0.4	11.9 ± 1.4
	O. glaberrima	11.9 ± 3.5	88.1 ± 3.5*	5.5 ± 1.1	9.7 ± 0.8
	O. sativa	14.8 ± 10.6	85.2 ± 10.6*	8.6 ± 2.6	8.8 ± 1.0
Panicoideae	*Oplismenus undulatifolius*	8.2 ± 9.1	91.8 ± 9.1*	13.1 ± 1.4	8.9 ± 0.8
	Panicum bisulcatum	32.4 ± 8.3	67.6 ± 8.3*	12.7 ± 4.1	8.7 ± 0.8
Pooideae	*Avena fatua*	34.1 ± 8.5	65.9 ± 8.5*	10.9 ± 3.5	18.7 ± 1.0
	Bromus catharticus	23.1 ± 3.6	76.9 ± 3.6*	12.4 ± 1.0	12.9 ± 0.4
	B. rigidus	38.9 ± 14.7	61.1 ± 14.7	16.5 ± 1.8	18.7 ± 0.8
	Lolium perenne	8.6 ± 2.2	91.4 ± 2.2*	15.7 ± 2.2	13.7 ± 0.9
	Triticum aestivum	14.3 ± 6.9	85.7 ± 6.9*	20.5 ± 2.3	18.4 ± 3.0

Notes. Values are means ± SD of three plants.
*indicate significant differences between the two positions of mitochondria ($p < 0.05$).
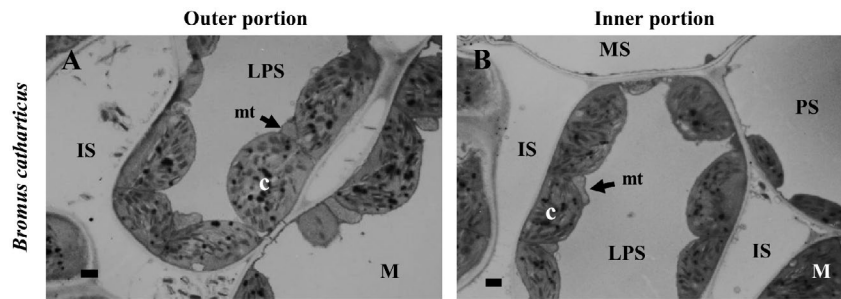
Figure 5. Ultrastructure of L-type parenchyma sheath cells in *B. catharticus*.

Notes. IS, intercellular space; LPS, L-type parenchyma sheath cell; M, mesophyll cell; MS, mestome sheath cell; PS, ordinary parenchyma sheath cell; c, chloroplast; mt, mitochondrion. Bars = 1 μm.

Table 3. Intracellular position and number of mitochondria and chloroplasts in L-type parenchyma sheath cells of C_3 species of the Pooideae.

Species	Mitochondria			Chloroplasts(number per cell profile)
	Outer position (%)	Inner position (%)	Number per cell profile	
Avena fatua	24.4 ± 7.8	75.6 ± 7.8*	8.7 ± 0.9	11.4 ± 0.5
Bromus catharticus	17.9 ± 19.2	82.1 ± 19.2*	6.8 ± 1.0	11.1 ± 1.8
B. rigidus	47.1 ± 17.1	52.9 ± 17.1	8.9 ± 4.1	10.4 ± 0.6
Lolium perenne	31.6 ± 8.9	68.4 ± 8.9*	7.1 ± 0.6	9.5 ± 1.9
Triticum aestivum	12.0 ± 2.8	88.0 ± 2.8*	11.0 ± 1.2	12.7 ± 1.0

Notes. Values are means ± SD of three plants.
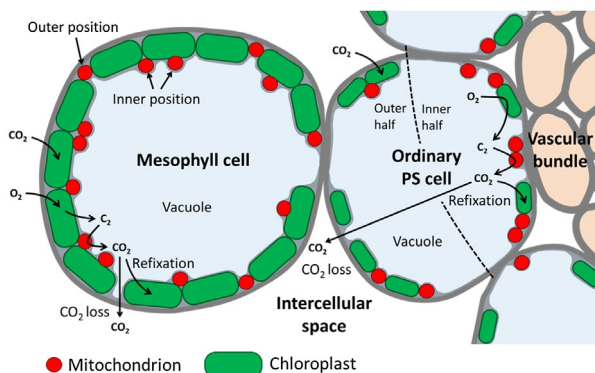*indicate significant differences between the two positions of mitochondria ($p < 0.05$).

Figure 6. Intracellular positions of mitochondria and chloroplasts and carbon flow in photosynthesis and photorespiration in ordinary parenchyma sheath and mesophyll cells of C_3 grasses.

Notes. C_2 indicates a two-carbon photorespiratory metabolite. PS, parenchyma sheath.

between PS cells and vascular bundle cells. These mitochondria may have high respiratory activity to supply energy for metabolite transport (O'Brien & Carr, 1970). Currently, it is unclear whether the positioning of organelles found in the PS cells of C_3 grasses is widespread in other C_3 species. However, at least the proto-Kranz grass species such as *Steinchisma laxa* (formerly *Panicum laxum*) and *Panicum hylaeicum* (Brown et al., 1983; Sage et al., 2014) have increased proportions of centripetal mitochondria and chloroplasts in the PS cells. Subsequently, C_3–C_4 intermediate species such as *Steinchisma hians* (formerly

Panicum milioides) might evolve with increased proportions of centripetal mitochondria and chloroplasts and exclusive expression of GDC in PS mitochondria (Gowik & Westhoff, 2011; Sage et al., 2014).

In the PS of the Pooideae and Panicoideae, a band around the vascular bundle representing the accumulation of GDC was more prominent than in the PS of the Ehrhartoideae. In light of the results of electron microscopy, the difference in the intensity of this band is likely caused by a higher total number of mitochondria rather than a higher proportion of centripetal mitochondria. The PS cells of Ehrhartoideae appear to contain fewer organelles than those of the Pooideae and Panicoideae, although the difference in the size of PS cells between species should also be considered. Whether the quantitative difference in organelles of PS cells reflects some physiological characteristics of each subfamily is unknown.

In the Pooideae, the PS cells on the xylem side were ordinary, whereas those on the phloem side were structurally similar to mesophyll cells. Williams et al. (1989) named these cells in barley the L-type PS cells. In our study, the number and intracellular position of organelles in L-type PS cells were similar to those in mesophyll cells, indicating an alteration of PS cells to mesophyll cells on the phloem side in the C_3 species of the Pooideae. The BS in C_3 plants is thought to have various physiological roles (Griffiths et al., 2013; Leegood, 2008; Sage, 2001), and C_3 species of the Pooideae would be an interesting model to study BS function in C_3 plants.

Intracellular position of mitochondria and chloroplasts in mesophyll cells

Many mitochondria were positioned on the vacuole side of chloroplasts (Figure 6), although there was no significant difference in the distribution of mitochondria between the outer and inner positions in the mesophyll cells of *B. rigidus*, where the gaps between chloroplasts were relatively large and held many mitochondria. In mesophyll cells of *Oryza* species and *O. undulatifolius*, stromules extended along the cell wall, and many mitochondria were positioned on the vacuole side of chloroplasts and stromules; this position might help rubisco in chloroplasts including stromules to refix photorespiratory (and respiratory) CO_2 released from mitochondria before it is lost outside mesophyll cells (Bourett et al., 1999; Buchner et al., 2015; Sage & Sage, 2009). Previous studies also examined the ultrastructure of mesophyll cells of C_3 grasses (Bourett et al., 1999; Gielwanowska et al., 2005; Lütz & Engel, 2007; Sage & Sage, 2009; Stata et al., 2014; Winter et al., 1993). In their electron micrographs, we can find the inner positioning of mitochondria as reported in our study. However, all the studies excluding the study on rice by Sage and Sage (2009) made no mention of this positioning.

In rice and wheat, Busch et al. (2013) reported that 24–38% of photorespired and respired CO_2 is reassimilated in mesophyll cells, the periphery of which is covered by chloroplasts and stromules; this reassimilation boosts photosynthesis by 8–11%. Busch et al. (2013) measured S_c/S_m, which was calculated as the length of cell periphery facing the intercellular air space covered by chloroplasts (S_c) divided by the total length of cell periphery facing the intercellular air space (S_m) in mesophyll cells and used as a structural parameter that affects CO_2 flux in chloroplasts. The value of intracellular positioning of mitochondria measured in our study could be used as a structural parameter indicating CO_2 loss from mitochondria. Our data suggest that the mechanism of photorespiratory (and respiratory) CO_2 scavenging proposed for rice and wheat (Busch et al., 2013; Sage & Sage, 2009) may be extended to other C_3 grasses. The proportion of mitochondria located in the inner position in mesophyll cells did not largely differ between the C_3 grasses of the Ehrhartoideae and Panicoideae (68–92%), which occur mainly in tropical and subtropical regions, and those of the Pooideae (61–91%), which occur in cold temperate regions. Therefore, intracellular positioning of mitochondria in mesophyll cells is a likely mechanism to scavenge photorespiratory (and respiratory) CO_2 that is widespread in C_3 grasses and is not restricted to certain subfamilies. In the glycolate pathway, NH_4^+ is also released during glycine decarboxylation in mitochondria (Keys et al., 1978; Leegood et al., 1995). Most NH_4^+ is incorporated in the glutamine synthetase–glutamate synthase cycle in chloroplasts, but some may be lost from leaves (Kumagai et al., 2011). Intracellular positioning of mitochondria may also reduce NH_4^+ emission.

In this study, we examined plants grown under optimum thermal conditions; the C_3 species of the Ehrhartoideae and Panicoideae were grown under summer conditions, whereas those of the Pooideae were under spring conditions. However, plant mitochondria can move in response to environmental stimuli, including light (Islam et al., 2009; Logan & Leaver, 2000). The development of stromules is also affected by environmental factors (Buchner et al., 2015; Moser et al., 2015; Yamane et al., 2012). Whether the intracellular positioning of mitochondria found in this study is changed by environmental factors that affect photorespiratory activity, such as light intensity, temperature, and CO_2 concentration, will be the topic of our future study.

Disclosure statement

Funding

References

Bauwe, H. (2011). Photorespiration: The bridge to C_4 photosynthesis. In A. S. Raghavendra & R. F. Sage (Eds.), C_4 *photosynthesis and related CO_2 concentrating mechanisms* (pp. 81–108). Heidelberg-Berlin: Springer Verlag.

Bourett, T. M., Czymmek, K. J., & Howard, R. J. (1999). Ultrastructure of chloroplast protuberances in rice leaves preserved by high pressure freezing. *Planta, 208*, 472–479. doi:10.1007/s004250050584.

Brown, R. H., Bouton, J. H., Rigsby, L., & Rigler, M. (1983). Photosynthesis of grass species differing in carbon dioxide fixation pathways : VIII. Ultrastructural characteristics of *Panicum* species in the Laxa group. *Plant Physiology, 71*, 425–431. doi:10.1104/pp.71.2.425

Brown, W. V. (1975). Variations in anatomy, associations, and origins of Kranz tissue. *American Journal of Botany, 62*, 395–402. doi:2442093

Buchner, O., Moser, T., Karadar, M., Roach, T., Kranner, I., & Holzinger, A. (2015). Formation of chloroplast protrusions and catalase activity in alpine *Ranunculus glacialis* under elevated temperature and different CO_2/O_2 ratios. *Protoplasma, 252*, 1613–1619. doi:10.1007/s00709-015-0778-5

Busch, F. A., Sage, T. L., Cousins, A. B., & Sage, R. F. (2013). C_3 plants enhance rates of photosynthesis by reassimilating photorespired and respired CO_2. *Plant, Cell and Environment, 36*, 200–212. doi:10.1111/j.1365-3040.2012.02567.x

Carolin, R. C., Jacobs, S. W. L., & Vesk, M. (1973). The structure of the cells of the mesophyll and parenchymatous bundle sheath of the Gramineae. *Botanical Journal of the Linnean Society, 66*, 259–275. doi:10.1111/j.1095-8339.1973.tb02174.x

Chonan, N. (1970). Studies on the photosynthetic tissues in the leaves of cereal crops. V. Comparison of the mesophyll structure among seedling leaves of cereal crops. *Japanese Journal of Crop Science, 39*, 418–425. doi:10.1626/jcs.39.418

Chonan, N., Kawahara, H., & Matsuda, T. (1974). Morphology on vascular bundles of leaves in gramineous crops. I. Observations on vascular bundles of leaf blades, sheaths and internodes in rice plants. *Japanese Journal of Crop Science, 43*, 425–432. doi:10.1626/jcs.43.425

Douce, R., Bourguignon, J., Neuburger, M., & Rébeillé, F. (2001). The glycine decarboxylase system: A fascinating complex. *Current Opinion in Plant Biology, 2*, 214–222. doi:10.1016/S1360-1385(01)01892-1

Edwards, E. J., & Smith, S. A. (2010). Phylogenetic analyses reveal the shady history of C_4 grasses. *Proceedings of the National Academy of Sciences, 107*, 2532–2537. doi:10.1073/pnas.0909672107

Edwards, G. E., & Ku, M. S. B. (1987). Biochemistry of C_3–C_4 intermediates. In M. D. Hatch & N. K. Boardman (Eds.), *Biochemistry of plants: Photosynthesis* (pp. 275–325). San Diego, CA: Academic Press.

Ehleringer, J. R., Sage, R. F., Flanagan, L.B., & Pearcy, R. W. (1991). Climate change and the evolution of C_4 photosynthesis. *Trends in Ecology and Evolution, 6*, 95–99. doi:10.1016/0169-5347(91)90183-X

Gielwanowska, I., Szczuka, E., Bednara, J., & Gorecki, R. (2005). Anatomical features and ultrastructure of *Deschampsia antarctica* (Poaceae) leaves from different growing habitats. *Annals of Botany, 96*, 1109–1119. doi:10.1093/aob/mci262

Gowik, U., & Westhoff, P. (2011). The path from C_3 to C_4 photosynthesis. *Plant Physiology, 155*, 56–63. doi:10.1104/pp.110.165308

Grass Phylogeny Working Group. (2001). Phylogeny and subfamilial classification of the grasses (Poaceae). *Annals of the Missouri Botanical Garden, 88*, 373–457. doi:10.2307/3298585

Gray, J. C., Sullivan, J. A., Hibberd, J. M., & Hansen, M. R. (2001). Stromules: Mobile protrusions and interconnections between plastids. *Plant Biology, 3*, 223–233. doi:10.1055/s-2001-15204

Griffiths, H., Weller, G., Toy, L. F. M., & Dennis, R. J. (2013). You're so vein: Bundle sheath physiology, phylogeny and evolution in C_3 and C_4 plants. *Plant, Cell and Environment, 36*, 249–261. doi:10.1111/j.1365-3040.2012.02585.x

Hatch, M. D. (1987). C_4 photosynthesis: a unique blend of modified biochemistry, anatomy and ultrastructure. *Biochimica et Biophysica Acta (BBA) - Reviews on Bioenergetics, 895*, 81–106. doi:10.1016/S0304-4173(87)80009-5

Islam, M. S., Niwa, Y., & Takagi, S. (2009). Light-dependent intracellular positioning of mitochondria in *Arabidopsis thaliana* mesophyll cells. *Plant and Cell Physiology, 50*, 1032–1040. doi:10.1093/pcp/pcp054

Kaneko, M., Chonan, N., Matsuda, T., & Kawahara, H. (1980). Ultrastructure of the small vascular bundles and transfer pathways for photosynthate in the leaves of rice plant. *Japanese Journal of Crop Science, 49*, 42–50. doi:10.1626/jcs.49.42

Keys, A. J., Bird, I. F., Cornelius, M. J., Lea, P. J., Wallsgrove, R. M., & Miflin, B. J. (1978). Photorespiratory nitrogen cycle. *Nature, 275*, 741–743. doi:10.1038/275741a0

Kumagai, E., Araki, T., Hamaoka, N., & Ueno, O. (2011). Ammonia emission from rice leaves in relation to photorespiration and genotypic differences in glutamine synthetase activity. *Annals of Botany, 108*, 1381–1386. doi:10.1093/aob/mcr245

Leegood, R. C., Lea, P. J., Adcock, M. D., & Häusler, R. E. (1995). The regulation and control of photorespiration. *Journal of Experimental Botany, 46*, 1397–1414. doi:10.1093/jxb/46.special_issue.1397

Leegood, R. C. (2008). Roles of the bundle sheath cells in leaves of C_3 plants. *Journal of Experimental Botany, 59*, 1663–1673. doi:10.1093/jxb/erm335

Logan, D. C., & Leaver, C. J. (2000). Mitochondria-targeted GFP highlights the heterogeneity of mitochondrial shape, size and movement within living plant cells. *Journal of Experimental Botany, 51*, 865–871. doi:10.1093/jexbot/51.346.865

Lütz, C., & Engel, L. (2007). Changes in chloroplast ultrastructure in some high-alpine plants: Adaptation to metabolic demands and climate. *Protoplasma, 231*, 183–192. doi:10.1007/s00709-007-0249-8

Monson, R. K., & Rawsthorne, S. (2000). CO_2 assimilation in C_3–C_4 intermediate plants. In R. C. Govindjee, J. Amesz, & E.-M. Aro (Eds.), *Photosynthesis: physiology and metabolism* (pp. 533–550). Dordrecht: Kluwer Academic.

Moser, T., Holzinger, A., & Buchner, O. (2015). Chloroplast protrusions in leaves of *Ranunculus glacialis* L. respond significantly to different ambient conditions, but are not related to temperature stress. *Plant, Cell and Environment, 38*, 1347–1356. doi:10.1111/pce.12483

Muhaidat, R., Sage, T. L., Frohlich, M. W., Dengler, N. G., & Sage, R. F. (2011). Characterization of C_3–C_4 intermediate species in the genus *Heliotropium* L. (Boraginaceae): Anatomy, ultrastructure and enzyme activity. *Plant, Cell and Environment, 34*, 1723–1736. doi:10.1111/j.1365-3040.2011.02367.x

O'Brien, T. P., & Carr, D. J. (1970). A suberized layer in the cell walls of the bundle sheath of grasses. *Australian Journal of Biological Sciences, 23*, 275–288. doi:10.1071/BI9700275

Rawsthorne, S. (1992). C_3–C_4 intermediate photosynthesis: Linking physiology to gene expression. *The Plant Journal, 2*, 267–274. doi:10.1111/j.1365-313X.1992.00267.x

Sage, R. F. (2001). Environmental and evolutionary preconditions for the origin and diversification of the C_4 photosynthetic syndrome. *Plant Biology, 3*, 202–213. doi:10.1055/s-2001-15206

Sage, T. L., Busch, F. A., Johnson, D. C., Friesen, P. C., Stinson, C. R., Stata, M., … Sage, R. F. (2013). Initial events during the evolution of C_4 photosynthesis in C_3 species of Flaveria. *Plant Physiology, 163*, 1266–1276. doi:10.1104/pp.113.221119

Sage, R. F., Khoshravesh, R., & Sage, T. L. (2014). From proto-Kranz to C_4 Kranz: Building the bridge to C_4 photosynthesis. *Journal of Experimental Botany, 65*, 3341–3356. doi:10.1093/jxb/eru180

Sage, T. L., & Sage, R. F. (2009). The functional anatomy of rice leaves: Implications for refixation of photorespiratory CO_2 and efforts to engineer C_4 photosynthesis into rice. *Plant and Cell Physiology, 50*, 756–772. doi:10.1093/pcp/pcp033

Stata, M., Sage, T. L., Rennie, T. D., Khoshravesh, R., Sultmanis, S., Khaikin, Y., … Sage, R. F. (2014). Mesophyll cells of C_4 plants have fewer chloroplasts than those of closely related C_3 plants. *Plant, Cell & Environment, 37*, 2587–2600. doi:10.1111/pce.12331

Ueno, O. (2011). Structural and biochemical characterization of the C$_3$–C$_4$ intermediate *Brassica gravinae* and relatives, with particular reference to cellular distribution of Rubisco. *Journal of Experimental Botany, 62*, 5347–5355. doi:10.1093/jxb/err187

Ueno, O., Bang, S. W., Wada, Y., Kondo, A., Ishihara, K., Kaneko, Y., & Matsuzawa, Y. (2003). Structural and biochemical dissection of photorespiration in hybrids differing in genome constitution between *Diplotaxis tenuifolia* (C$_3$–C$_4$) and radish (C$_3$). *Plant Physiology, 132*, 1550–1559. doi:10.1104/pp.103.021329

Vogan, P. J., Frohlich, M. W., & Sage, R. F. (2007). The functional significance of C$_3$-C$_4$ intermediate traits in *Heliotropium* L. (Boraginaceae): Gas exchange perspectives. *Plant, Cell and Environment, 30*, 1337–1345. doi:10.1111/j.1365-3040.2007.01706.x

Voznesenskaya, E. V., Koteyeva, N. K., Akhani, H., Roalson, E. H., & Edwards, G. E. (2013). Structural and physiological analyses in Salsoleae (Chenopodiaceae) indicate multiple transitions among C$_3$, intermediate, and C$_4$ photosynthesis. *Journal of Experimental Botany, 64*, 3583–3604. doi:10.1093/jxb/ert191

Williams, M. L., Farrar, J. F., & Pollock, C. J. (1989). Cell specialization within the parenchymatous bundle sheath of barley. *Plant, Cell and Environment, 12*, 909–918. doi:10.1111/j.1365-3040.1989.tb01970.x

Winter, H., Robinson, D. G., & Heldt, H. W. (1993). Subcellular volumes and metabolite concentrations in barley leaves. *Planta, 191*, 180–190. doi:10.1007/BF00199748

Yamane, K., Mitsuya, S., Taniguchi, M., & Miyake, H. (2012). Salt-induced chloroplast protrusion is the process of exclusion of ribulose-1,5-bisphosphate carboxylase/oxygenase from chloroplasts into cytoplasm in leaves of rice. *Plant, Cell and Environment, 35*, 1663–1671. doi:10.1111/j.1365-3040.2012.02516.x

Yoshimura, Y., Kubota, F., & Ueno, O. (2004). Structural and biochemical bases of photorespiration in C$_4$ plants: Quantification of organelles and glycine decarboxylase. *Planta, 220*, 307–317. doi:10.1007/s00425-004-1335-1